Boswellic acid and myrrh sesquiterpene alleviate hypoxic-ischemic brain injury via regulating TLR4/NF-κB and Ang □/Ang □/Tie signaling pathway on MCAO rats

Xiaodong Miao
Nanjing University of Chinese Medicine
Zizhang Zhao
Nanjing University of chinese medicine
Zhuo Xu
Nanjing University of chinese medicine
Shulan Su (sushulan1974@163.com)
Nanjing University of chinese medicine
Baoping Jiang
Nanjing University of Chinese Medicine
Er-xin Shang
Nanjing University of chinese medicine
Jiashang Li
Nanjing University of chinese medicine
Yue Zhu
Nanjing University of Chinese Medicine
Jianming Guo
Nanjing University of Chinese Medicine
Li Yu
Nanjing University of chinese medicine
Dawei Qian
Nanjing University of Chinese Medicine
Jin-ao Duan
Nanjing University of Chinese Medicine

Research

Keywords: ischemic stroke, middle cerebral artery occlusion, boswellic acid, myrrh sesquiterpenes, metabolomics analysis, gut microbiota

Posted Date: November 12th, 2020

DOI: https://doi.org/10.21203/rs.3.rs-105919/v1

Abstract

Background: The frankincense and myrrh can be used in traditional Chinese medicine (TCM) clinic with the treatment of stroke, while its mechanism is still unclear. The aim of this study was to investigate the effects of boswellic acid (BA) and myrrh sesquiterpene (MS) compositions on ischemic stroke in rats.

Methods: The ischemic stroke rat model induced by ischemia-reperfusion (I/R) after transient middle cerebral artery occlusion (MCAO) was adopted and treated with boswellic acid and myrrh sesquiterpenes with proportions compatibility (BA-MS) of 10:1, 5:1 and 20:1. Biochemical indexes, histopathological analysis, metabolomics analysis of plasma and urine, as well as 16S rDNA sequencing of gut microbiota and short chain fatty acids were investigated.

Results: BA and MS could obviously significantly ameliorated neurological deficits scores, reduced cerebral infarction area in I/R, and improve the damage of brains and lungs of MCAO rats. Additionally, it could significantly reduce the expression of neuroinflammatory factors (IL-1β, nNOS, BDNF, NGF) and angiogenic growth factors (ET-1, PAI-1, PDGF, VEGF, VWF), and significantly increase the expression of nerve indicators (TDP-43, NeuN) and angiogenic growth factors (Ang □, TGF-β1, bFGF). After the administration of BA-MS, the metabolites of ischemic stroke in plasma and urine of ischemic stroke of rats were reversed, mainly correlated with the metabolic pathway of linoleic acid metabolism (impact value =1), and the gut microbiota and SCFAs metabolism of cecal contents were also improved.

Conclusions: BA-MS can improve brain injury of MCAO rats via Ang/Tie and TLR4 signaling pathway, improve metabolism disorder by regulating linoleic acid metabolism pathway, and ameliorate gut microbes and their metabolic disorders.

1. Background

In 2017, stroke became the leading cause of death in China [1]. It is clinically divided into ischemic stroke and hemorrhagic stroke, among which, ischemic stroke accounts approximately 80%. Ischemic stroke is devastating and caused by thromboembolic occlusion of the cerebral aorta or its branches [2]. The victim may suddenly experience paralysis, speech problems or vision loss [3]. The risk factors of ischemic stroke are various. Some are unchangeable, while some can be adjusted to reduce the risk, like hypertension [4], diabetes [5], dyslipidemia [6], etc. Cerebral ischemia reperfusion (I/R) injury is mediated by multiplex mechanisms. Vascular obstruction not only leads to the loss of oxygen and energy, which followed by the formation of reactive oxygen species, the release of glutamic acid, the accumulation of intracellular calcium, but also induces neuroinflammation [7]. The series of reactions eventually leads to brain injury or even brain death, and infections may occur, especially in the lungs [8]. Therefore, inhibiting the development of neuroinflammation [9] and stimulating angiogenesis [10, 11] are the key to recovering the brain's focal I/R response.

Currently, thrombolytic therapy is a powerful clinical treatment for ischemic stroke [12]. The standard method is to use of an enzyme tissue plasminogen activator (t-PA), which lyses plasminogen and

converts it into active thrombolytic plasminogen [13]. However, using t-PA has limitations, including complications of intracranial hemorrhage. Traditional Chinese medicine has been used in the clinical treatment of cerebrovascular diseases for a long time known as little side effects and multiple targets [14].

Frankincense is a gelatinous resin exuded from *Boswellia carterii* Birdw. or *Boswellia bhaw-dajiana* Birdw. Myrrh is an oily gelatinous substance exuded from the bark of *Commiphora myrrh* Engl. or *Commiphora molmo*l Engl. Frankincense and myrrh (FM) are typical Chinese medicine pair, which have the effects of activating blood and removing stasis, astringent wound, and generating muscle. Boswellic acids (BA) and myrrh sesquiterpenes (MS) are respectively the main bioactive compound in frankincens and myrrh. Previous studies found that the most common ratios of FM were 1:1, 1:2, and 2:1, and then converted them to the ratio of 10:1, 5:1, 20:1 of BA-MS according to their respective extraction rates [15]. In addition, modern studies have shown that adding frankincense when treating of stroke patients can effectively improve muscle weakness and non-dominant muscle strength in patients with acute neurological dysfunction [16]. The oil extracted by mixing white pepper, long pepper, myrrh, cinnamon and saffron in a conventional ratio of 1:2:2:2:2 (w/w) protected PC12 cells from oxygen glucose deprivation [17]. So BA-MS has the potential to treat ischemic stroke, while the unclear mechanism limits its clinical application.

In this study, we examined the effects of different proportions of BA-MS on I/R in MCAO rats through pathological sections, biochemical indicators, metabolomics analysis, intestinal flora diversity analysis, short chain fatty acids (SCFAs) analysis, and comprehensive correlation analysis between biochemical indicators and metabolites, intestinal flora and SCFAs to understand the potential mechanism of oral BA-MS in the treatment of ischemic stroke.

2. Materials And Methods

2.1 Materials

Frankincense (lot 171010) and myrrh (lot 171108) were purchased from Suzhou Tianling Chinese Herbal Medicine Co., Ltd., the processing method is vinegar. ACQUITY UPLC System (Waters, USA), Xevo mass spectrometer (Waters), MassLynx mass spectrometry workstation software (Waters). perkinelmer clams 680 series connection flame ionization detector (FID). Tissue homogenizer (DHS Life Science & Technology Co., Ltd. Beijing, China), ultrasonic cell disrupter (Ningbo Scientz Biotechnology Co., Ltd. Ningbo, China), shaking table (Qilinbeier Instrument Co., Ltd. Haimen, China), high speed refrigeration centrifuge (Thermo), full-wavelength microplate reader (Thermo).Others materials see Supplementary.

2.2 Preparation of drug solution [15]

The preparation of BA and MS see Supplementary. BA and MS were freeze-dried and stored, the compatibility ratio of FM (1:1, 1:2, 2:1) were converted to about BA-MS (10:1, 5:1, 20:1) according to the extraction rate, and the specific dose was shown in **2.3**.

2.3 Animal experiment

Animal protocol was approved by the Institutional Animal Ethics Committee of Nanjing University of Chinese Medicine. SD rats were fed conventional feeding and water freely. Temperature and humidity were maintained at 23 ± 2 °C and 60 ± 2%, respectively, and the light cycle was 12 h.

After adaptive feeding period, the fasted (12 h) rats were anesthetized with 10% chloral hydrate via intraperitoneally injection (400 mg/kg) and placed on warm pads to maintain the body temperature at 37 ± 1 °C throughout the whole procedure. The left common carotid artery, external carotid artery and internal carotid artery were exposed and then a line with rounded ends was used to close the middle cerebral artery (MCA). The wire passed from the external carotid artery to the internal carotid artery lumen for 17 to 20 mm until resistance was felt to ensure occlusion at the origin of the MCA. The line was allowed to stay there for 120 minutes before gently retracting. The rats of sham group were performed by the method of MCAO without inserting the line. All the animals were scored 1–5 for neurological function 3 h after surgery by people who did not know the experimental group, until specimens were taken. 1–4 points can be classified as successful modeling. Scoring criteria see Supplementary.

Successful modeling rats were randomly divided into nine groups: sham group (n = 7), model group (M, n = 12), Nimodipine group (YXY, 21.6 mg/kg/d, n = 9), the ratio of BA and MS was 10:1 with high dose and low dose groups (H10:1, BA: 720 mg/kg/d, MS: 72 mg/kg/d; L10:1, BA: 180 mg/kg/d, MS: 18 mg/kg/d, n = 9), the ratio of BA and MS was 5:1 with high dose and low dose groups (H5:1, BA: 475.2 mg/kg/d, MS: 95.04 mg/kg/d; L5:1, BA: 118.8 mg/kg/d, MS: 23.76 mg/kg/d, n = 9) and the ratio of BAand MS was 20:1 with high dose and low dose groups (H20:1, BA: 950.4 mg/kg/d, MS: 47.52 mg/kg/d; L20:1, BA: 237.6 mg/kg/d, 11.88 mg/kg/d, n = 9). Then twice per day, 10 mL/kg was given by gavage each time. All rats were administrated daily at scheduled time for 3 consecutive days. For sham and model groups rats were given physiological saline undergoing the same procedure.

At the end of treatment, 12-hour urine was collected with metabolic cage and all rats were anaesthetized (10% chloral hydrate) after overnight-fasted. Plasma was collected and centrifuged (3000 r/min, 10 min). The left ventricle was perfused with saline until the effluent from the right ventricular ear became colorless and the liver color became white. The brains, lungs, thymus and spleens were quickly taken, weighed, and viscera index was calculated (viscera index = viscera weight (g)/rat weight (g) × 100%). A portion of the brains and lungs were placed in formalin and the rest in liquid nitrogen and then stored at -80 °C for further study. The collected cecum contents were stored at -80 °C for 16 s rDNA sequencing and short-chain fatty acids analysis.

2.4 Longa neurological scores and weight changes

Longa neurological scores were performed at 24 h, 48 h, and 72 h after I/R. Daily and 24 h weight after surgery was recorded, change in body weight was calculated, and neurological function was scored 3 h after surgery by people who did not know the experimental grouping during until the whole experiment. Change in body weight (%) = (body weight at each time point - body weight before surgery)/ body weight before surgery × 100%.

2.5 Measure infarct size and general histology

2.5.1 TTC staining

Fresh brain was removed and then cut into 2 mm coronal sections and immediately incubated with 2% 2,3, 5-triphenyl-tetrazolium chloride (TTC, Solarbio, lot. G3005) at 37 °C for 15 minutes. The tissue was gently shaken at intervals of 5–8 min to evenly contact the staining solution, then the reaction was terminated by adding a stationary solution (Solarbio, lot. p1110). Image J software was used to quantitatively analyze the infarct area.

2.5.2 HE staining

Brains and lungs tissue were removed and dehydrated with 4% paraformaldehyde solution fixed with tissue, embedded in paraffin and cut into 4 μm. And observed under 200 × by optical microscope after the sections were stained with hematoxylin and eosin (H&E).

2.6 Biochemical indicators

The contents of IL-1β, nNOS, BDNF, NGF, ET-1, VEGF, PDGF, Ang □, PAI-1 in the plasma were estimated by ELISA kits (Nanjing Jiancheng Bioengineering Institute, China).

2.7 IHC staining

The immobilized brain tissue was pretreated with paraffin sectioning, then antigen repaired, inactivated enzyme by 3% H_2O_2-methanol solution, and incubated with rabbit-anti- TDP-43 (1:100, abcam ab109535, UK), rabbit-anti- NeuN (1:1000, abcam ab177487, UK), mouse-anti-TGF-β1 (1:100, abcam ab190503, UK), rabbit-anti- VWF (1:100,SANTA sc-14014, USA), rabbit-anti- bFGF(1:100, bs-0217R, China) after sealed by using 1% BSA. Then, sheep anti-rabbit/rat polymer was added for primary and secondary antibody reaction, and color rendering by DAB solution, color rendering by distilled water was stopped, hematoxylin dye was re-dyed, dehydrated and sealed, and protein expression in tissue cells was observed under 400x optical microscope.

2.8 Protein expression analysis

Protein was extracted from the injured side of the brains by homogenization, and protein concentration was determined with the BCA protein concentration determination kit (solabal, Beijing, China). Inactivated enzyme after adjusting the protein concentration, followed by gel preparation, sample loading, electrophoresis, membrane transfer, sealing and incubation of primary antibodies (NF-κB, 1:1000, CST; p-NF-κB, 1:1000, CST; TLR4, 1:500, proteintech; Ang □, 1:1000, proteintech; Ang □, 1:1000, proteintech; Tie2, 1:1000, proteintech; and β-actin, 1:10 000, CST). After 4 °C for the night, incubation two resistance (1:30 00). Finally, X film is used in the darkroom to sensitize, develop and fix after the membrane reacts with ECL chemiluminescence solution (Tanon).

2.9 Metabolomics study on plasma and urine

The plasma and urine were thawed at room temperature before preparation, and were extracted with three times of acetonitrile to precipitate protein, respectively. Then, the mixture was swirled for 30 seconds and centrifuged at 13,000 rpm for 15 minutes at 4 °C. The samples was redissolved using 50% acetonitrile

(2:1) after centrifugally concentrated, and then 2 μL was injected into UPLC-MS for metabolic analysis. Quality control sample, liquid phase conditions and mass spectrometry conditions see Supplementary.

2.10 Intestinal microecology analysis

2.10.1 Gut flora diversity analysis

Extract total DNA from cecum contents samples according to E.Z.N.A. soil kit instructions. The concentration and purity of DNA were determined by NanoDrop2000, and the quality of DNA was determined by 1% agarose gel electrophoresis. The variable region of V3-V4 was amplified by 338F (5'-ACTCCTACGGGAGGCAGCAG-3') and 806R (5'-GGACTACHVGGGTWTCTAAT-3') primers. PCR products were recovered by 2% agarose gel, purified by AxyPrep DNA gel extraction kit (Axygen, USA), eluded by Tris-HCl, and detected by 2% agarose gel electrophoresis. QuantiFluor™ -ST (Promega, USA) was used for quantitative testing. PE*2 × 300 library was constructed according to Illumina MiSeq platform (Illumina, USA) standard operating procedure. The original sequence was controlled by Trimmomatic software and assembled by FLASH software. According to the similarity of 97%, will not repeat sequence (not including single sequence) according to operating classification unit (OTU) clustering, get OTU the representation of the sequence using UPARSE (vsesion 7.0 http://drive5.com/uparse/) software. The abundance and diversity of the single-sample microbial community were reflected by Alpha dilution curve analysis. In addition, at the phylum level to genus level, linear discriminant analysis (LDA) was conducted and Linear discrimination analysis effect size (LEfSe) software was used to identify the species with significant differences on sham group and model group. Finally, the function of the 16S amplicon was predicted by PICRUSt.

2.10.2 Metabolites of intestinal flora analysis

Sample treatment: 100 mg of cecum contents thawed on ice were added to 4 × methanol homogenate, centrifuged at 13 000 rpm for 10 min. Supernatant redissolved and transferred to a liquid bottle after centrifuged and concentrated, and 2 μL of sample was injected for GC-FID analysis.

Reference solution: acetic acid (lot H1808008), propionic acid (lot. A1903124), butyric acid (lot.D1917157), isobutyric acid (lot.K1822187), valeric acid (lot.G1818016), isovaleric acid (lot C1919091) were purchased from Aladdin (Darmstadt, Germany, purity > 99.5%). They were dissolved with methanol to concentration of 52.25 mg/mL, 50.34 mg/mL, 44.37 mg/mL, 47.24 mg/mL, 45.19 mg/mL, 44.37 mg/mL, respectively, then diluted by 2 times, 4 times, 8 times, 16 times, 32 times, 64 times and 128 times. Gas chromatographic condition see Supplementary.

2.11 Statistical analysis

All data were statistically analyzed by Graphpad 7, The results were expressed as mean ± SD. The one-way ANOVA was used for comparison between groups. A P value < 0.05 was regarded as significant.

3. Results

3.1 Effects of nerve function, body weight and visceral indexes

There was a significant decrease in body weight between M group and the sham group at 24 h, 48 h and 72 h after I/R after operation. At each time point, it showed no significant difference, but a decreasing trend can be seen (Fig. 1a). The neurological function score showed there were different degrees of improvement after 72 h of administration (Fig. 1b). Viscera index (Fig. 1c) showed that brain, lung and spleen indexes increased significantly in M group compared with the sham group, while thymus index decreased significantly.

3.2 Effects of BA-MS on cerebral infarct area and general histology

As shown in Fig. 2a, viable tissue was deep red by TTC staining, whereas area of infarction in the injured side cerebral hemisphere was white. The brain infarction area in M group was significantly increased in comparison to the sham group ($P < 0.001$). Compared with M group, 20:1 group showed the smallest infarction area ($P < 0.001$), followed by 5:1 group ($P < 0.01$) and H10:1 group ($P < 0.01$). In addition, the brains of the rats in M group exhibited an edematous morphology with neuron loss and pyknotic nuclei in H&E staining, and this condition was effectively ameliorated in each treatment group (Fig. 2b). The lungs of the rats in M group appeared pulmonary bullae with alveolar structure damaged. Alveolar capillary wall thickened and infiltrated the alveolar space and peribronchi in H&E staining, which was consistent with the development of pulmonary infection in rats after stroke [18, 19], and it was effectively ameliorated in treatment groups (Fig. 2c).

3.3 BA-MS improved biochemical indexes

The results of biochemical indexes were shown in Fig. 2d. M group showed significant increase in IL-1β, nNOS, BDNF, NGF, ET-1, PAI-1, PDGF-BB and VEGF-A levels, as well as a significant decrease in Ang□ level in comparison with sham group. After the administration, the above indicators all tended to be normal. H5:1 group and H20:1 group were generally better than other administration groups.

As shown in Fig. 3a and Fig. 3b, the expressions of bFGF, TGF-β1 and vWF were significantly increased and TDP-43, NeuN were significantly decreased in cerebral I/R region after MCAO. Compared with M group, administration groups had obviously increased the expressions of bFGF, TGF-β1, TDP-43 and NeuN, while remarkably decreased the expressions of vWF.

3.5 Effects of BA-MS on protein expressions of NF-κB, p-NF-κB, TLR4, Ang□, Ang□ and Tie2 in Western blot analysis

Western blotting results (Fig. 3c) showed that the expression of NF-κB, p-NF-κB and TLR4 protein in cerebral I/R region after MCAO were significantly increased, and Ang□, Ang□ and Tie2 protein were significantly decreased compared with the sham group ($P < 0.05$). In general, the H20:1, H10:1 and H5:1 had significant effects on the expression of NF-κB, p-NF-κB, TLR4, Ang□, Ang□ and Tie2, and H5:1 showed the best regulatory effect.

3.6 Metabolism analysis

The OPLS-DA score plots (**Figure S1a**) showed that sham and M group could be clearly separated, indicating that metabolic disorders occurred in the model group. PCA score (**Figure S1b**) showed that the plasma and urine samples of sham and M group had significant clustering. The administration groups deviated from M group and was closer to the sham operation group, indicating the drug administration groups could improve the metabolic disorder of I/R in MCAO rats. In the *S*-plot plot (**Figure S1c**), metabolites that deviate from the main ion cluster and VIP ≥ 1 was extracted as differential metabolites. Then, 21 potential biomarkers (**Table S1**, among them 9 from plasma and 12 from urine.) and 16 potential metabolism pathways (impact ≥ 0.1) were identified by HMDB (www.hmdb.ca) and Metabo Analyst (http://www.metaboanalyst.ca/) database. As shown in **Figure S1d**, the occurrence of I/R in MCAO rats may be associated with retinol metabolism, pentose and glucuronate interconversions, linoleic acid metabolism, glycerophospholipid metabolism, biotin metabolism, ascorbate and aldarate metabolism, phenylalanine metabolism, terpenoid backbone biosynthesis, pantothenate and CoA biosynthesis, ether lipid metabolism, sphingolipid metabolism, pyruvate metabolism, galactose metabolism, cysteine and methionine metabolism, arachidonic acid metabolism and steroid hormone biosynthesis. Among them, linoleic acid metabolism had an impact-value of 1, which suggested the administration of BA-MS could modify this metabolic pathways and be related biomarkers to exert the curative effect for I/R after MCAO rats. The results also showed BA-MS could improve metabolic disorders in I/R after MCAO by regulating metabolites. Other details see **Figure S2**.

3.7 Regulation of BA-MS on intestinalmicroecology

3.7.1 Gut microbiota analysis

In order to investigate whether the therapeutic effect of the bioactive parts of BA-MS in different proportions on I/R after MCAO was related to intestinal flora, we analyzed the cecum contents flora of rats after 72 h of treatment and the species diversity of the sample at OTU level. **Figure S3** showed the sample length distribution was in the range of 400 to 440 bp. Sobs index was to measure colony richness, Heip index was to measure colony evenness, and Shannon index was to evaluate species diversity of the samples at OUT level, as shown in **Figure S4a**. The results showed that there were high richness, diversity and uniformity of the microflora in each group, and there was no significant difference in the diversity index. Dilution curve (**Figure S4b)**, showed that the current sequencing depth was enough to reflect the diversity contained in the current sample, and a large number of undiscovered new OTU cannot be detected by increasing the sequencing depth. In addition, the number of each sample at the level of phylum and genus was counted. At the phylum level **(**Fig. 4a**)**, *firmicutes*, *proteobacteria*, *bacteroidetes* and *verruciformis* were found after the combination of species with abundance less than 0.1%, and *Firmicutes* accounted for the largest proportion. At the genus level **(**Fig. 4a**)**, *escherichia-shigella*, *allobaculum*, norank_f_*muribaculaceae*, *akkermansia*, *lactobacillus*, *prevotella*_9 were found after the combination of species with abundance less than 0.1%. According to the LEfSe multi-species hierarchy tree diagram **(**Fig. 4b**)**, compared with the normal group, the intestinal flora of the model group was different in phylum, class, order, family and genus. The Linear discriminant analysis (LDA) discriminant bar graph **(**Fig. 4b**)** was made from phylum level to genus level. By comparing the sham

group with M group and Welch's t test, significant differences were found in 3 phylums and 27 genus. It was found that H5:1 significantly increased the relative abundance of *actinobacteria* and *tenericutes* at the phylum level (Fig. 4c**)**. The administration groups could regulate 10 species of bacteria at the genus level, among which H5:1 had the best effect, followed by H10:1, H20:1, L10:1 and YXY. Further studies showed that the intestinal flora of I/R in MCAO rats were involved in 24 related functions (**Figure S5**) and metabolic pathways of the top 20 abundance values (**Table S2**). Among them, amino acid transport and metabolism, cell wall/membrane/envelope biogenesis, replication, recombination and repair, ribosomal structure and biogenesis, energy production and conversion have high functional abundance, and carbohydrate metabolism, amino acid metabolism, replication and repair, energy metabolism, nucleotide metabolism and lipid metabolism pathways disorder contribute directly or indirectly to the development of ischemia stroke.

3.7.2 Short-chain fatty acids analysis

In order to investigate the effects of different proportions of BA-MS bioactive ingredients on intestinal flora metabolites in I/R rats, we analyzed SCFAs in cecum contents of rats after 72 h of I/R. The chromatogram of the mixed reference substances, sham and M groups was shown in **Figure S6**, and the precision, stability, repeatability, average recovery and linear relation of six SCFAs components were shown in **Table S3**. It can be seen in Fig. 4d, compared with the sham group, the contents of acetic acid and propionic acid in the caecum of M group were significantly decreased, and the contents of each administration group were increased to different degrees. H5:1 had a significant effect on the contents of acetic acid and propionic acid in the contents of the I/R rats' cecum after MCAO, suggesting that H5:1 could improve the effect of ischemic stroke by increasing the content of SCFAs in the contents of the cecum of MCAO rats.

3.8 Correlation analysis

It can be seen from the heat map of correlation analysis (Fig. 5a), NeuN was positively correlated with PM5 and PM9 ($r > 0.7$); PDGF-BB was positively correlated with UN2 ($r > 0.7$); Ang was correlated with UN6 ($r > 0.7$); p-NF-κB was negatively correlated with PM5 ($r < -0.7$); TDP-43 was positively correlated with PM6 ($r > 0.7$), VWF was negatively correlated with PM1 ($r < -0.7$).

Correlation analysis heat maps of the above gut microbes and SCFAs were carried out. In this experiment, the Pearson correlation coefficients $r > 0.4$ and $r<-0.4$ respectively indicate medium positive correlation and medium negative correlation. The correlation of unclassified_ks-k_*dbacteria*, *verrucomicrobia* and *cyanobacteria* were good at the phylum level (Fig. 5b). There were 15 good correlations at the genus level (Fig. 5b), *lachnospiraceae*_NK4A136_group, *clostridium*_sensu_stricto_1, *lactobacillus*, norank_f_*Lachnospiraceae*, *bifidobacterium*, *streptococcus*, *akkermansia*, *turicibacter*, norank_o_*gastranaerophilales*, *proteus*, *parasutterella*, norank_f_*erysipelotrichaceae*, [*eubacterium*]_*coprostanoligenes*_group, *phascolarctobacterium*, *butyricimonas*.

4. Discussion

Currently, a variety of animal stroke models have been developed to identify the mechanisms of cerebral ischemia and developing new treatments for stroke [2]. Middle cerebral artery (MCA) and its branches are the most common cerebral blood vessels in human ischemic stroke, thus, the technique to block the artery is closest to a human ischemic stroke [2]. In occlusive MCA stroke models, intra-arterial suture blockade of MCA (MCAO) is the most common method in rodents [20]. Therefore, in this study, the MCAO rat model of I/R was established to evaluate the therapeutic effect of BA-MS with different compatibility ratios on ischemic stroke, and to clarify the mechanism.

When cerebral ischemia occurs, a decrease in blood flow due to arterial occlusion will lead to hypoxia, which quickly induce neurological deficits or death. And it not only changes the ultrastructure and function of the brain [10], but also affects the function of the lung [21]. Post stroke pulmonary infection was found to be the result of bacterial flora displacement due to the destruction of the intestinal barrier after stroke [22]. In addition, after ischemic stroke, microglia and astrocytes are activated within a few hours, producing cytokines and chemokines [23] and causing the infiltration of white blood cells [24], suggesting that secondary neuroinflammation further promotes brain damage [25]. In our study, the administration groups were shown to improve neurological function, cerebral infarction area, and brain and lung morphology; as well as modulate anti-inflammatory factors (IL-1β, nNOS), neurotrophic factors (BDNF, NGF), and angiogenic growth factors (ET-1, VEGF, PDGF, Ang □, PAI-1).

The sequelaes of ischemic stroke include language barrier, limb muscle atrophy and so on. Recent studies suggest that TDP-43 may be pathological marker proteins for neurodegenerative diseases such as amyotrophic lateral sclerosis (ALS) [26, 27] and frontotemporal lobar degeneration (FTLD) [28]. In the pathological case, TDP-43 accumulates from the nucleus to the cytoplasm, causing a decrease of TDP-43 in the nucleus [29]. This explains the significant reduction of TDP-43 in M group compared to the sham group, and the significant callback in the administration groups (L5:1, YXY). NeuN is a soluble nuclear protein, a marker for mature neurons [30]. Our results showed that NeuN positive expression was significantly decreased in M group, and NeuN positive cell expression was significantly increased in administration groups (20:1, H10:1, YXY) compared with the sham group. This suggests that the administration groups improved ischemic stroke by inducing NeuN expression. TGF-β1, VWF, and bFGF are important regulators of angiogenesis. Our results also demonstrated that BA-MS can promote angiogenic growth by improving TGF-β1, VWF and bFGF. In addition, western blot results showed that the TLR4/NF-κB and Ang □, Ang □/Tie2 signaling pathways were activated after I/R. TLR4 is a member of the toll-like receptor family and can activate downstream NF-κB and participates in inflammatory responses [31]. Ang □, Ang □ and their receptors Tie2 are related to a new angiogenesis signal pathway discovered in recent years, except for vascular endothelial growth factor (VEGF) [32]. Studies have shown that the combination of Ang □ and the receptor activates Tie2, and Tie2-activated endothelial cells form a complete vascular wall, thus promoting angiogenesis and maintaining the stability of vascular structure [33, 34]. BA-MS may improve damaged brains by inhibiting inflammatory responses and promoting angiogenic growth.

Metabolomics is a systematic approach to the study of metabolic changes. By analyzing the composition and changes of endogenous metabolites in biological samples, the physiological and pathological state of the subjects was explained to reflect the overall metabolic law under the influence of internal and external factors [35]. Metabolomics results showed that the impact value of linoleic acid metabolic pathway was 1, indicating that BA-MS interfered with the occurrence of ischemic stroke by regulating linoleic acid metabolism. Moreover, the correlation analysis of metabolic markers and biochemical indicators also showed that linoleic acid was strongly negatively correlated with IL-1β (r= -0.641) and VWF (r=-0.606). It also found that the content of linoleic acid, which is essentially a polyunsaturated fatty acid, decreased in the M group. Therefore, we speculated that the decrease of linoleic acid was closely related to the increase of IL-1β and VWF after stroke. Studies have found that substituting linoleic acid for saturated fats, glycemic carbohydrates, or monounsaturated fats may reduce the risk of ischemic stroke [36], possibly because linoleic acid lowers plasma low density lipoprotein cholesterol levels [37].

The balance of intestinal flora is critical to the normal development of the immune system [38]. Intestinal microorganisms interact with the host, providing energy, nutrition and immune protection to the host against disease, as well as producing toxins that affect the health of the host [39]. Many diseases associated with abnormal microbes have an "inflammatory" basis, from autoimmune diseases to atherosclerotic heart disease, high blood pressure and even stroke [40]. SCFAs are metabolites of intestinal microorganisms, mainly including acetic acid, propionic acid and butyric acid. And it may have important associations with diet, gut flora, and inflammatory responses [41]. The correlation between gut microbiota and SCFAs showed that isovaleric acid was positively correlated with norank_f_*Lachnospiraceae*, *Clostridium*_sensu_surico_1 ($r \geq 0.4$); acetic acid was positively correlated with *Lactobacillus* ($r \geq 0.4$), and acetic acid, propionic acid and butyric acid were negatively correlated with *Parasutterella* ($r \leq -0.4$). This was consistent with callback the gut microbial in I/R rats after administration groups, suggesting that the decrease of those flora disrupts the balance of the intestinal environment, thus exacerbating the progression of ischemic stroke, which was effectively improved in the administration groups.

Hyperglycemia is one of the important causes of ischemic stroke [5], report found that the advanced-stage diabetic rats have the characteristics of cognitive impairment, its relative abundance of gut microbes showed *Lachnospiraceae*_NK4A136_group increased, while the relative abundance of *Clostridium*_sensu_stricto_1 reduced [42]. *Lachnospiraceae* is a butyrate producing bacteria in *firmicutes* [43], and butyrate is an anti-inflammatory short-chain fatty acid salt that can provide nutrition for intestinal mucosa and enhance intestinal mucosal immunity [44]. *Lactobacillus* can reduce plasma endotoxin [45] and inhibit inflammatory response [46]. *Parasutterella* is related to irritable bowel syndrome and chronic intestinal inflammation [47]. Compared with the sham group, the relative abundance of *Parasutterella* increased significantly in M group, while *Lactobacillus* and norank_f_*Lachnospiraceae* decreased. In addition, there has been evidence that the imbalance of intestinal flora after stroke can aggravate the cerebral infarction area [48, 49]. So we suspected that after brain injury, the increase in *Parasatella* and the decrease in *Lactobacillus* and *Lachnospiraceae* leads to

intestinal inflammatory response, which in turn exacerbates brain injury. After administration, it was found that administration groups significantly increased the relative abundance of *Lactobacillus* and norank_f_*Lachnospiraceae*, and significantly reduced the relative abundance of *Parasatella*, suggesting that BA-MS may reduce the incidence of ischemic stroke by improving the inflammatory response of intestinal microorganisms through the "brain-gut axis".

5. Conclusion

In general, BA-MS can improve brain and lung injury of MCAO rats, which may alleviate nerve inflammation and promote angiogenesis growth by regulating TLR4/NF-κB signaling pathways and Ang □/Ang □/Tie signaling pathway, improve metabolism disorder by regulating linoleic acid metabolism pathway, and ameliorate gut microbes and their metabolic disorders. In terms of overall treatment effect, H5:1 has the best effect, followed by H10:1 and H20:1 (Fig. 6). The results of the study can provide beneficial inspiration for the treatment of ischemic stroke.

Abbreviations

MCAO: middle cerebral artery occlusion, I/R: ischemia-reperfusion, SCFAs: short chain fatty acids, BA: boswellic acids, MS: myrrh sesquiterpenes, BA-MS: boswellic acid compatible with myrrh sesquiterpenes, IHC: immunohistochemical, IL-1β: Interleukin 1β, nNOS: Neuronal nitric oxide synthase, BDNF: brain-derived neurotrophic factor, NGF: nerve growth factor, TDP-43: TAR DNA/RNA binding protein 43, NeuN: neuron nuclear, ET-1: endothelin-1, VEGF: vascular endothelial growth factor, PDGF: platelet derived growth factor, Ang □: Angiogenin 2, PAI-1: plasminogen activator inhibitor 1, TGF-β1: Transforming growth factor-β1, VWF: von willebrand factor, bFGF: basic fibroblast growth factor, FM: Frankincense and myrrh, YXY: Nimodipine group, H10:1: the ratio of BA and MS was 10:1 with high dose group, L10:1□the ratio of BA and MS was 10:1 with low dose group, H5:1: the ratio of BA and MS was 5:1 with high dose group, L5:1: the ratio of BA and MS was 10:1 with low dose group, H20:1: the ratio of BAand MS was 20:1 with high dose group, L20:1: the ratio of BAand MS was 20:1 with low dose group.

Declarations

Availability of supporting data

The datasets used or analysed during the current study are available from the corresponding author on reasonable request.

Ethics approval and consent to participate

All the experiments involving animals were approved by the Institutional Animal Ethics Committee of Nanjing University of Chinese Medicine.

Consent for publication

Not applicable.

Competing interests

The authors declare that they have no competing interests.

Authors' contributions

Conceived and designed the experiments: MXD, SSL, DJA. Performed the experiments: MXD, ZZZ, XZ, LJS, JBP. Analyzed the data: MXD, ZZZ, XZ. Contributed reagents/materials/analysis tools: SEX, ZY, GJM, YL, QDW. Contributed to the writing of the manuscript: MXD, XZ, SSL. All authors read and approved the final manuscript.

Acknowledgments: The authors would like to thank all of the colleagues and students who contributed to this study.

Sources of Funding: This work was supported by the National Natural Science Foundation of China (No. 30973885; 81373889; 81673533; 81973708). This work was also financially supported by the Jiangsu Key Laboratory for High Technology Research of TCM Formulae Project (No. FJGJS-2015-12), Construction Project for Jiangsu Key Laboratory for High Technology of TCM Formulae Research (BM2010576).

References

1. Zhou M, Wang H, Zeng X, Yin P, Zhu J, Chen W, et al. Mortality, morbidity, and risk factors in China and its provinces, 1990–2017: a systematic analysis for the Global Burden of Disease Study 2017. Lancet. 2019;394:1145–58.
2. Fluri F, Schuhmann MK, Kleinschnitz C. Animal models of ischemic stroke and their application in clinical research. Drug Des Devel Ther. 2015;9:3445–54.
3. Moskowitz MA, Lo EH, Iadecola C. The science of stroke: Mechanisms in search of treatments. Neuron. 2010. p. 181–98.
4. Lawes CMM, Bennett DA, Feigin VL, Rodgers A. Blood Pressure and Stroke: An Overview of Published Reviews. Stroke. 2004. p. 776–85.
5. Rodgers A. Blood glucose and risk of cardiovascular disease in the Asia Pacific region. Diabetes Care. 2004;27:2836–42.
6. Holme I, Aastveit AH, Hammar N, Jungner I, Walldius G. Relationships between lipoprotein components and risk of ischaemic and haemorrhagic stroke in the Apolipoprotein MOrtality RISk study (AMORIS). J Intern Med. 2009;265:275–87.
7. Lipton P. Ischemic cell death in brain neurons. Physiol. Rev. 1999. p. 1431–568.
8. Shim R, Wong CHY. Ischemia, immunosuppression and infection-tackling the predicaments of post-stroke complications. Int. J. Mol. Sci. 2016. p. 1–18.

9. Tuttolomondo A, Di Raimondo D, Pecoraro R, Arnao V, Pinto A, Licata G. Inflammation in Ischemic Stroke Subtypes. Curr Pharm Des. 2012;18:4289–310.
10. Wan J, Wan H, Yang R, Wan H, Yang J, He Y, et al. Protective effect of Danhong Injection combined with Naoxintong Capsule on cerebral ischemia-reperfusion injury in rats. J Ethnopharmacol. 2018;211:348–57.
11. Heydenreich N, Nolte MW, Göb E, Langhauser F, Hofmeister M, Kraft P, et al. C1-inhibitor protects from brain ischemia-reperfusion injury by combined antiinflammatory and antithrombotic mechanisms. Stroke. 2012;43:2457–67.
12. Moussaddy A, Demchuk AM, Hill MD. Thrombolytic therapies for ischemic stroke: Triumphs and future challenges. Neuropharmacology. 2018. p. 272–9.
13. Hatcher MA, Starr JA. Role of tissue plasminogen activator in acute ischemic stroke. Ann Pharmacother. 2011;45:364–71.
14. Han JY, Li Q, Ma ZZ, Fan JY. Effects and mechanisms of compound Chinese medicine and major ingredients on microcirculatory dysfunction and organ injury induced by ischemia/reperfusion. Pharmacol. Ther. 2017. p. 146–73.
15. Miao X dong, Zheng L jie, Zhao Z zhang, Su S lan, Zhu Y, Guo J ming, et al. Protective effect and mechanism of boswellic acid and Myrrha sesquiterpenes with different proportions of compatibility on neuroinflammation by LPS-induced BV2 cells combined with network pharmacology. Molecules. 2019;24.
16. Jivad N, Rezaie Kheyrabadi F, Rafieyan M, Yarmohamadi samani P. A survey the clinical efficacy of frankincense in acute ischemic stroke. J Ilam Univ Med Sci. 2017;25:12–9.
17. Li J, Guan E, Chen L, Zhang X, Yin L, Dong L, et al. Optimization for extraction of an oil recipe consisting of white pepper, long pepper, cinnamon, saffron, and myrrh by supercritical carbon dioxide and the protective effects against oxygen–glucose deprivation in PC12 cells. Rev Bras Farmacogn. 2018;28:312–9.
18. Zhang SR, Nold MF, Tang SC, Bui CB, Nold CA, Arumugam T V., et al. IL-37 increases in patients after ischemic stroke and protects from inflammatory brain injury, motor impairment and lung infection in mice. Sci Rep. 2019;9.
19. Jin R, Zhu X, Liu L, Nanda A, Granger DN, Li G. Simvastatin attenuates stroke-induced splenic atrophy and lung susceptibility to spontaneous bacterial infection in mice. Stroke. 2013;44:1135–43.
20. Howells DW, Porritt MJ, Rewell SSJ, O'Collins V, Sena ES, Van Der Worp HB, et al. Different strokes for different folks: The rich diversity of animal models of focal cerebral ischemia. J. Cereb. Blood Flow Metab. 2010. p. 1412–31.
21. Hozawa A, Billings JL, Shahar E, Ohira T, Rosamond WD, Folsom AR. Lung function and ischemic stroke incidence: The atherosclerosis risk in communities study. Chest. 2006;130:1642–9.
22. Wen SW, Wong CHY. An unexplored brain-gut microbiota axis in stroke. Gut Microbes. 2017;8:601–6.
23. Perini F, Morra M, Alecci M, Galloni E, Marchi M, Toso V. Temporal profile of serum anti-inflammatory and pro-inflammatory interleukins in acute ischemic stroke patients. Neurol Sci. 2001;22:289–96.

24. Jin R, Yang G, Li G. Inflammatory mechanisms in ischemic stroke: role of inflammatory cells. J Leukoc Biol. 2010;87:779–89.
25. Jayaraj RL, Azimullah S, Beiram R, Jalal FY, Rosenberg GA. Neuroinflammation: Friend and foe for ischemic stroke. J. Neuroinflammation. 2019.
26. Gregory JM, McDade K, Bak TH, Pal S, Chandran S, Smith C, et al. Executive, language and fluency dysfunction are markers of localised TDP-43 cerebral pathology in non-demented ALS. J Neurol Neurosurg Psychiatry. 2019;
27. Maurel C, Madji-Hounoum B, Thepault RA, Marouillat S, Brulard C, Danel-Brunaud V, et al. Mutation in the RRM2 domain of TDP-43 in Amyotrophic Lateral Sclerosis with rapid progression associated with ubiquitin positive aggregates in cultured motor neurons. Amyotroph Lateral Scler Front Degener. 2018;19:149–51.
28. Dean PM, Smith GE, Parisi JE, Dickson DW, Petersen RC, Josephs KA. Neurocognitive speed associates with frontotemporal lobar degeneration TDP-43 subtypes. J Clin Neurosci. 2013;20:1737–41.
29. Ederle H, Dormann D. TDP-43 and FUS en route from the nucleus to the cytoplasm. FEBS Lett. 2017. p. 1489–507.
30. Qiao L, Fu J, Xue X, Shi Y, Yao L, Huang W, et al. Neuronalinjury and roles of apoptosis and autophagy in a neonatal rat model of hypoxia-ischemia-induced periventricular leukomalacia. Mol Med Rep. 2018;17:5940–9.
31. Faure E, Equils O, Sieling PA, Thomas L, Zhang FX, Kirschning CJ, et al. Bacterial lipopolysaccharide activates NF-κB through toll-like receptor 4 (TLR-4) in cultured human dermal endothelial cells. Differential expression of TLR-4 and TLR-2 in endothelial cells. J Biol Chem. 2000;275:11058–63.
32. Lund EL, Høg A, Olsen MWB, Hansen LT, Engelholm SA, Kristjansen PEG. Differential regulation of VEGF, HIF1α and angiopoietin-1, -2 and -4 by hypoxia and ionizing radiation in human glioblastoma. Int J Cancer. 2004;108:833–8.
33. Huang J, Inoue M, Hasegawa M, Tomihara K, Tanaka T, Chen J, et al. Sendai viral vector mediated angiopoietin-1 gene transfer for experimental ischemic limb disease. Angiogenesis. 2009;12:243–9.
34. Lee SW, Kim WJ, Jun HO, Choi YK, Kim KW. Angiopoietin-1 reduces vascular endothelial growth factor-induced brain endothelial permeability via upregulation of ZO-2. Int J Mol Med. 2009;23:279–84.
35. Connor SC, Hansen MK, Corner A, Smith RF, Ryan TE. Integration of metabolomics and transcriptomics data to aid biomarker discovery in type 2 diabetes. Mol Biosyst. 2010;6:909–21.
36. Venø SK, Schmidt EB, Jakobsen MU, Lundbye-Christensen S, Bach FW, Overvad K. Substitution of linoleic acid for other macronutrients and the risk of ischemic stroke. Stroke. 2017;48:3190–5.
37. Mensink RP, Zock PL, Kester ADM, Katan MB. Effects of dietary fatty acids and carbohydrates on the ratio of serum total to HDL cholesterol and on serum lipids and apolipoproteins: A meta-analysis of 60 controlled trials. Am J Clin Nutr. 2003;77:1146–55.
38. Kunz C, Kuntz S, Rudloff S. Intestinal flora. Adv Exp Med Biol. 2009. p. 67–79.

39. Brunkwall L, Orho-Melander M. The gut microbiome as a target for prevention and treatment of hyperglycaemia in type 2 diabetes: from current human evidence to future possibilities. Diabetologia. 2017. p. 943–51.
40. Gominak SC. Vitamin D deficiency changes the intestinal microbiome reducing B vitamin production in the gut. The resulting lack of pantothenic acid adversely affects the immune system, producing a “pro-inflammatory” state associated with atherosclerosis and autoimmun. Med Hypotheses. 2016;94:103–7.
41. Vinolo MAR, Ferguson GJ, Kulkarni S, Damoulakis G, Anderson K, Bohlooly-Y M, et al. SCFAs induce mouse neutrophil chemotaxis through the GPR43 receptor. PLoS One. 2011;6.
42. Gao H, Jiang Q, Ji H, Ning J, Li C, Zheng H. Type 1 diabetes induces cognitive dysfunction in rats associated with alterations of the gut microbiome and metabolomes in serum and hippocampus. Biochim Biophys Acta - Mol Basis Dis. 2019;1865.
43. Machiels K, Joossens M, Sabino J, De Preter V, Arijs I, Eeckhaut V, et al. A decrease of the butyrate-producing species roseburia hominis and faecalibacterium prausnitzii defines dysbiosis in patients with ulcerative colitis. Gut. 2014;63:1275–83.
44. Hamer HM, Jonkers D, Venema K, Vanhoutvin S, Troost FJ, Brummer RJ. Review article: The role of butyrate on colonic function. Aliment. Pharmacol. Ther. 2008. p. 104–19.
45. Nanji AA, Khettry U, Sadrzadeh SMH. Lactobacillus Feeding Reduces Endotoxemia and Severity of Experimental Alcoholic Liver (Disease). Proc Soc Exp Biol Med. 1994;205:243–7.
46. Karimi K, Inman MD, Bienenstock J, Forsythe P. Lactobacillus reuteri-induced regulatory T cells protect against an allergic airway response in mice. Am J Respir Crit Care Med. 2009;179:186–93.
47. Chen YJ, Wu H, Wu S Di, Lu N, Wang YT, Liu HN, et al. Parasutterella, in association with irritable bowel syndrome and intestinal chronic inflammation. J Gastroenterol Hepatol. 2018;33:1844–52.
48. Singh V, Roth S, Llovera G, Sadler R, Garzetti D, Stecher B, et al. Microbiota dysbiosis controls the neuroinflammatory response after stroke. J Neurosci. 2016;36:7428–40.
49. Winek K, Engel O, Koduah P, Heimesaat MM, Fischer A, Bereswill S, et al. Depletion of Cultivatable Gut Microbiota by Broad-Spectrum Antibiotic Pretreatment Worsens Outcome After Murine Stroke. Stroke. 2016;47:1354–63.

Figures

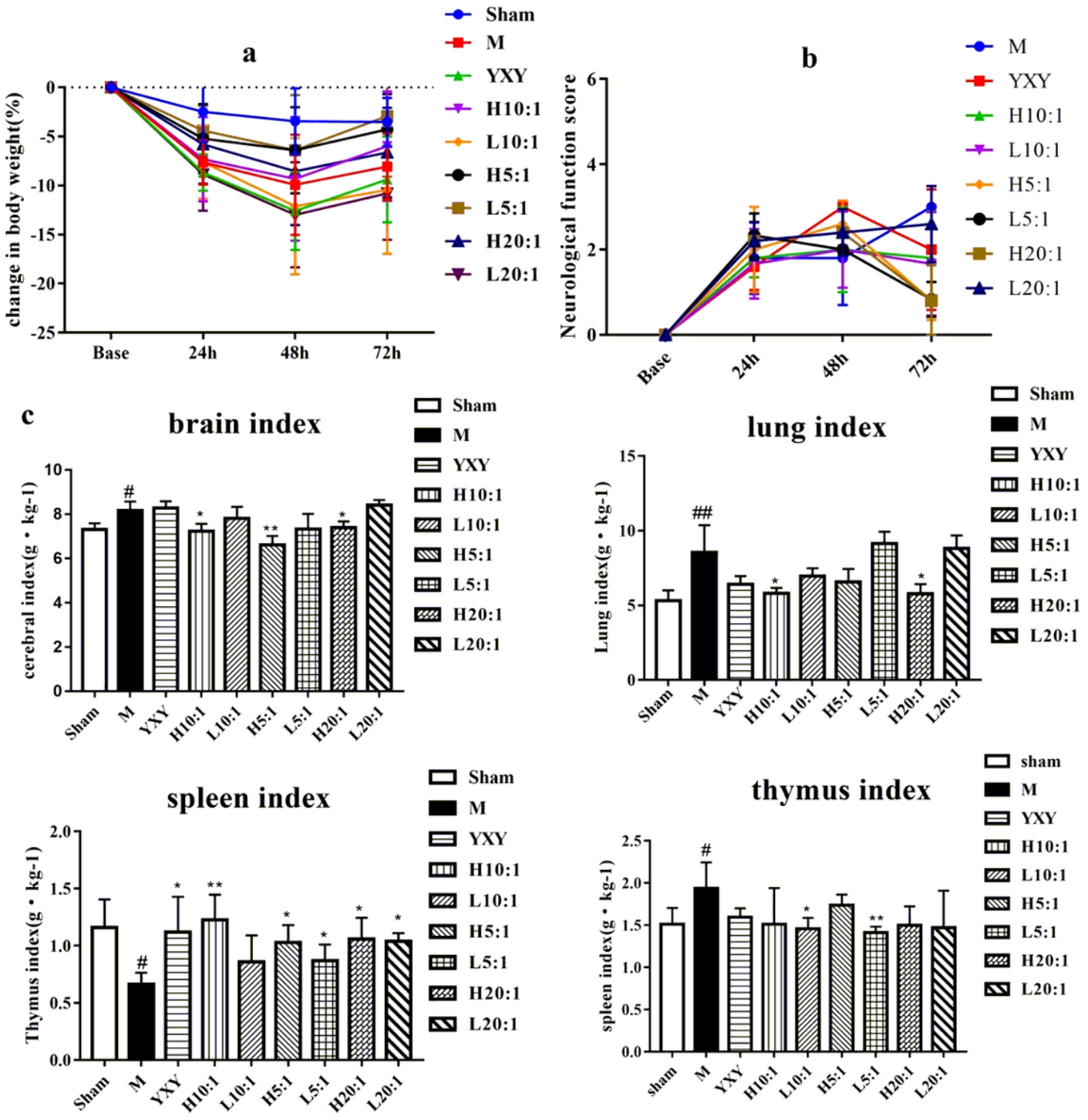

Figure 1

Neurological function score (a), Changes in body weight (b), Visceral Index of I/R after MACO rats. (c) (molde group vs sham group: #P < 0.05; ##P < 0.01, administration groups vs model group: *P < 0.05; **P < 0.01)

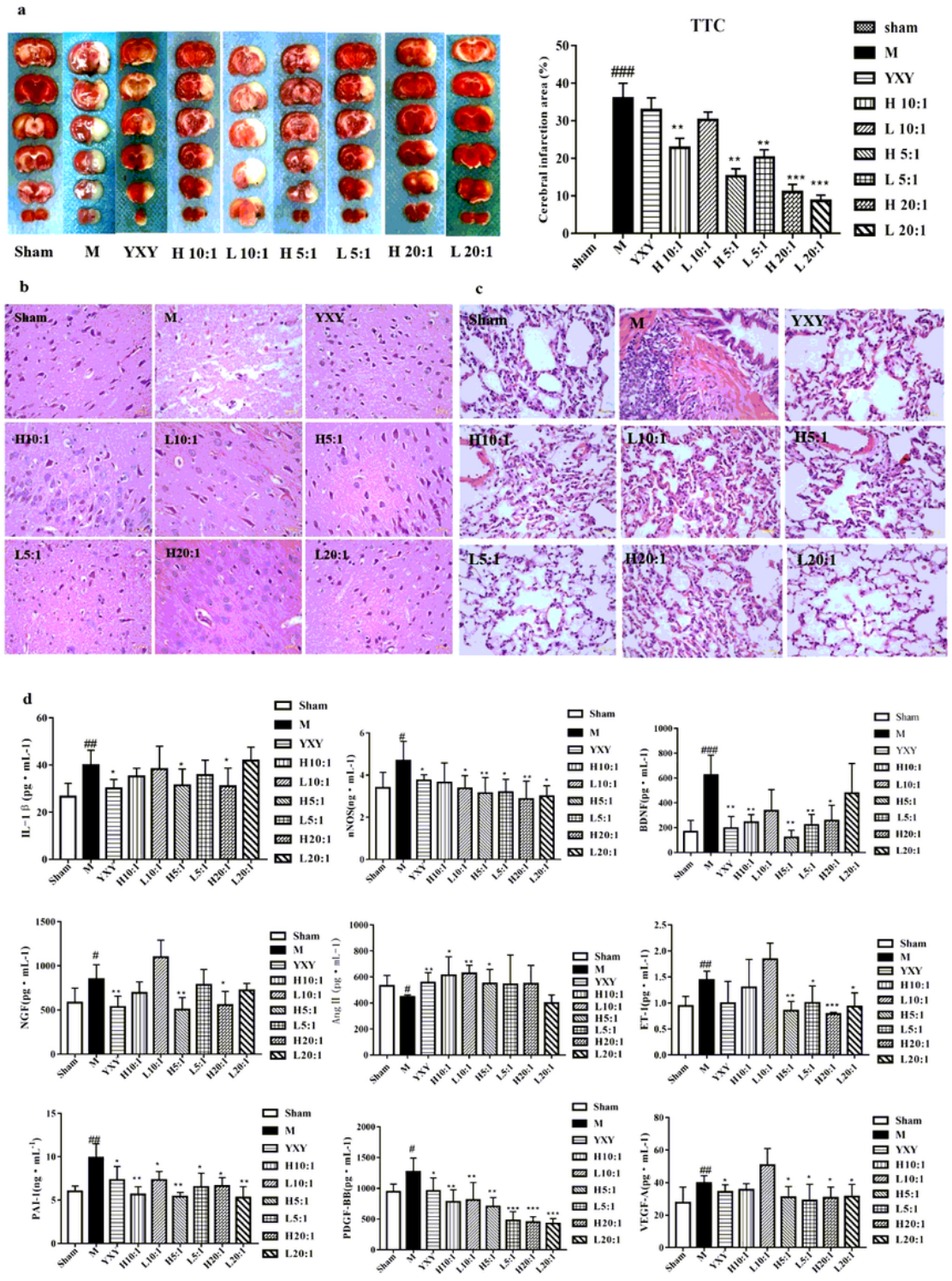

Figure 2

The effect of BA-MS on cerebral infarct volume in the focal cerebral I/R rats. (a) (molde group vs sham group: #P < 0.05; ##P < 0.01: ###P <0.001administration groups vs model group: *P < 0.05; **P < 0.01; ***P <0.001); Analysis of HE staining of brains (b) and lungs (c) (×400) among control group, model group and administration groups; Determination of IL-1β, nNOS, ET-1, PAI-1, PDGF-BB, VEGF-A, BDNF, NGF

and Ang among sham group, model group and administration groups.(d) (#P < 0.05; ##P < 0.01, model group vs sham group; *P < 0.05; **P < 0.01; ***P <0.001: administration groups vs model group.)

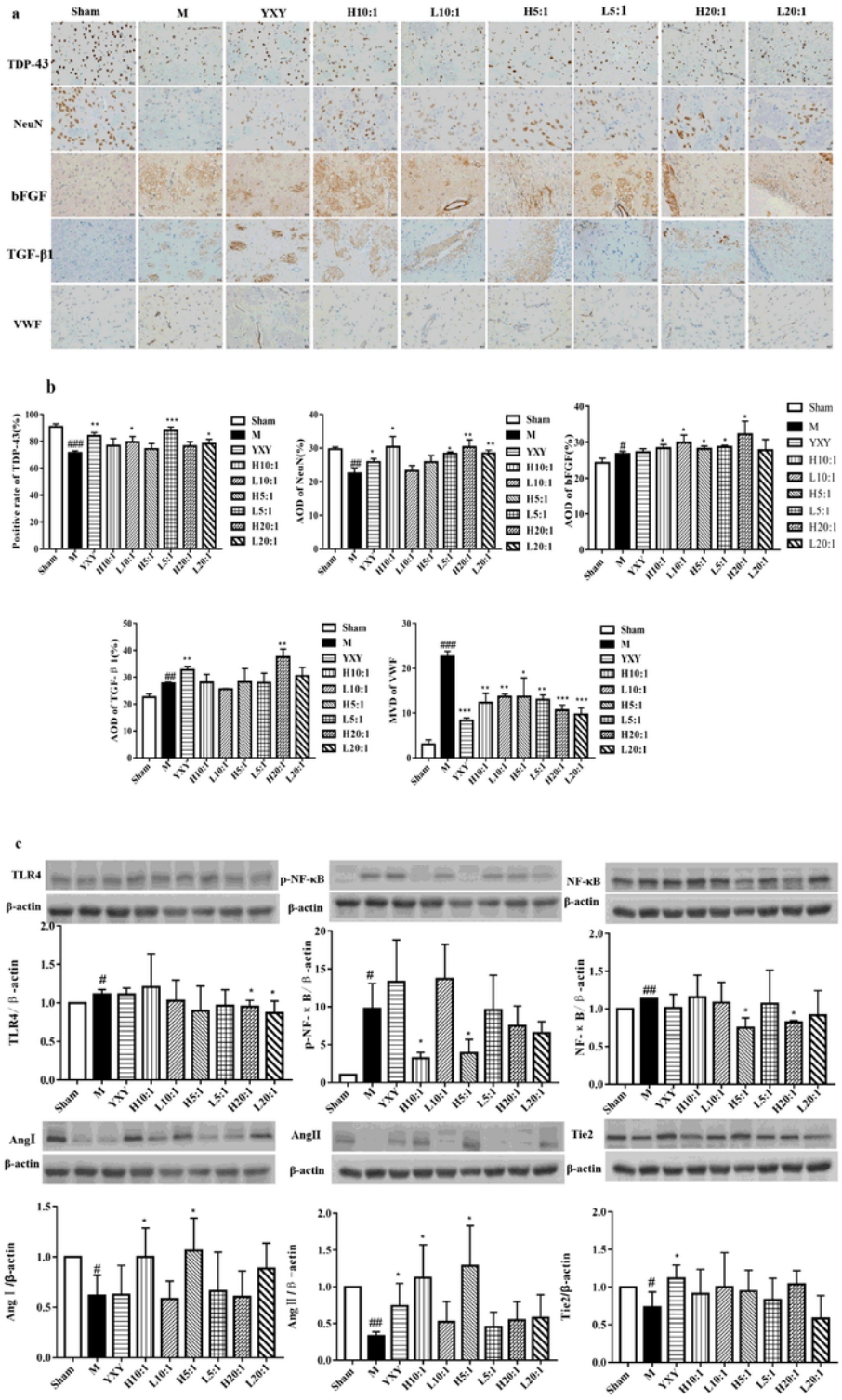

Figure 3

The TDP-43, NeuN, bFGF, TGF-β1, and vWF immunostained tissue of focal cerebral I/R rats (a) (200×). Immunohistochemical analysis of TDP-43, NeuN, bFGF, TGF-β1, and vWF in cerebral I/R region (b). (#P < 0.05; ##P < 0.01; ###P <0.001: model group vs sham group; *P < 0.05; **P < 0.01; ***P <0.001:

administration groups vs model group.); Western blotting determination of NF-κB, p-NF-κB, TLR4, Ang, Ang and Tie2 protein expression in cerebral I/R region.(c) (#P < 0.05: model group vs sham group; *P < 0.05; **P < 0.01: administration groups' vs model group.)

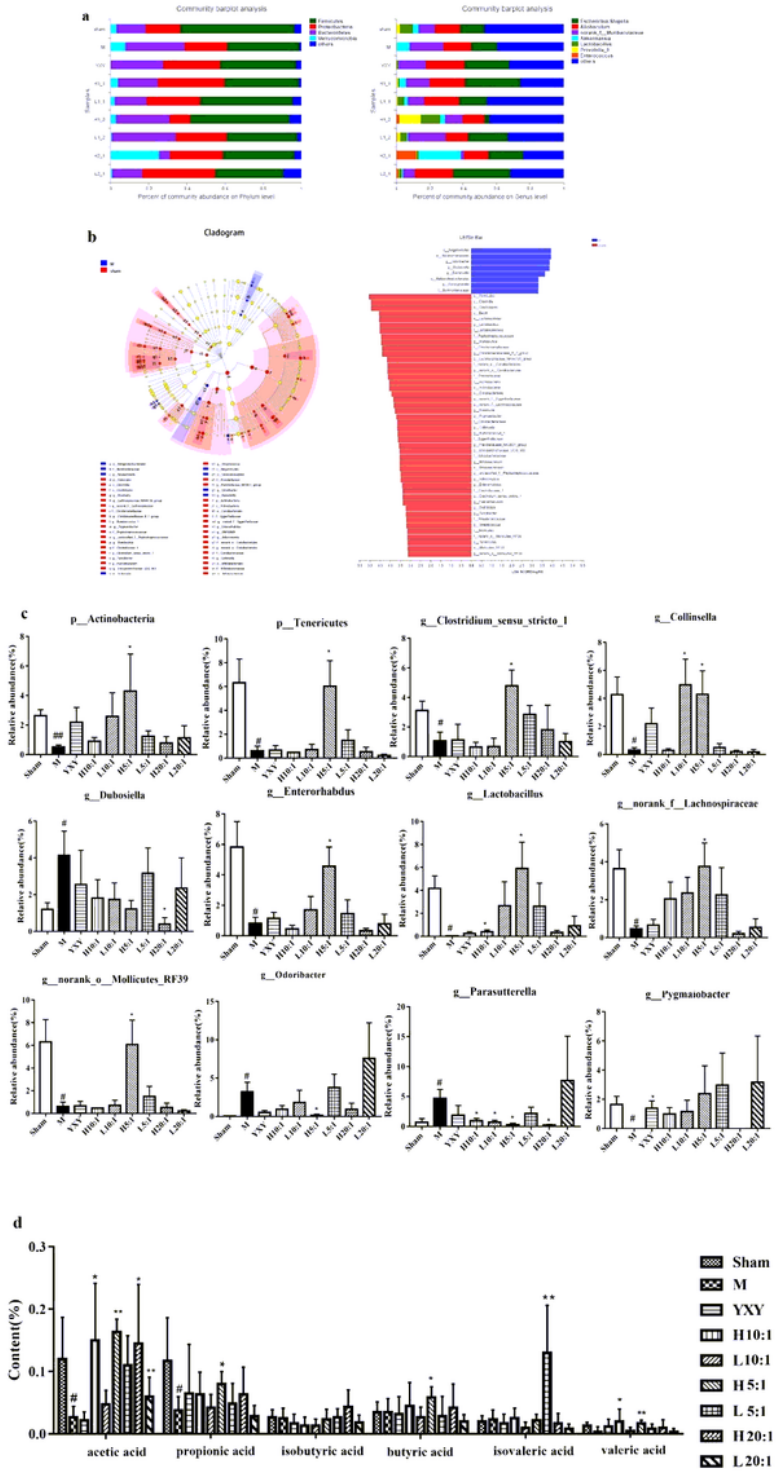

Figure 4

Community distribution at the phylum and genus level (a)(X-axis：Relative abundance ratio; Y-axis: Groups); LEfSe multilevel species hierarchy tree and LDA bar chart compared between the sham group

and the model group (b); the relative abundance of different species in each group (c). (#P < 0.05; ##P < 0.01: model group vs sham group; *P < 0.05; **P < 0.01: administration groups vs model group.)

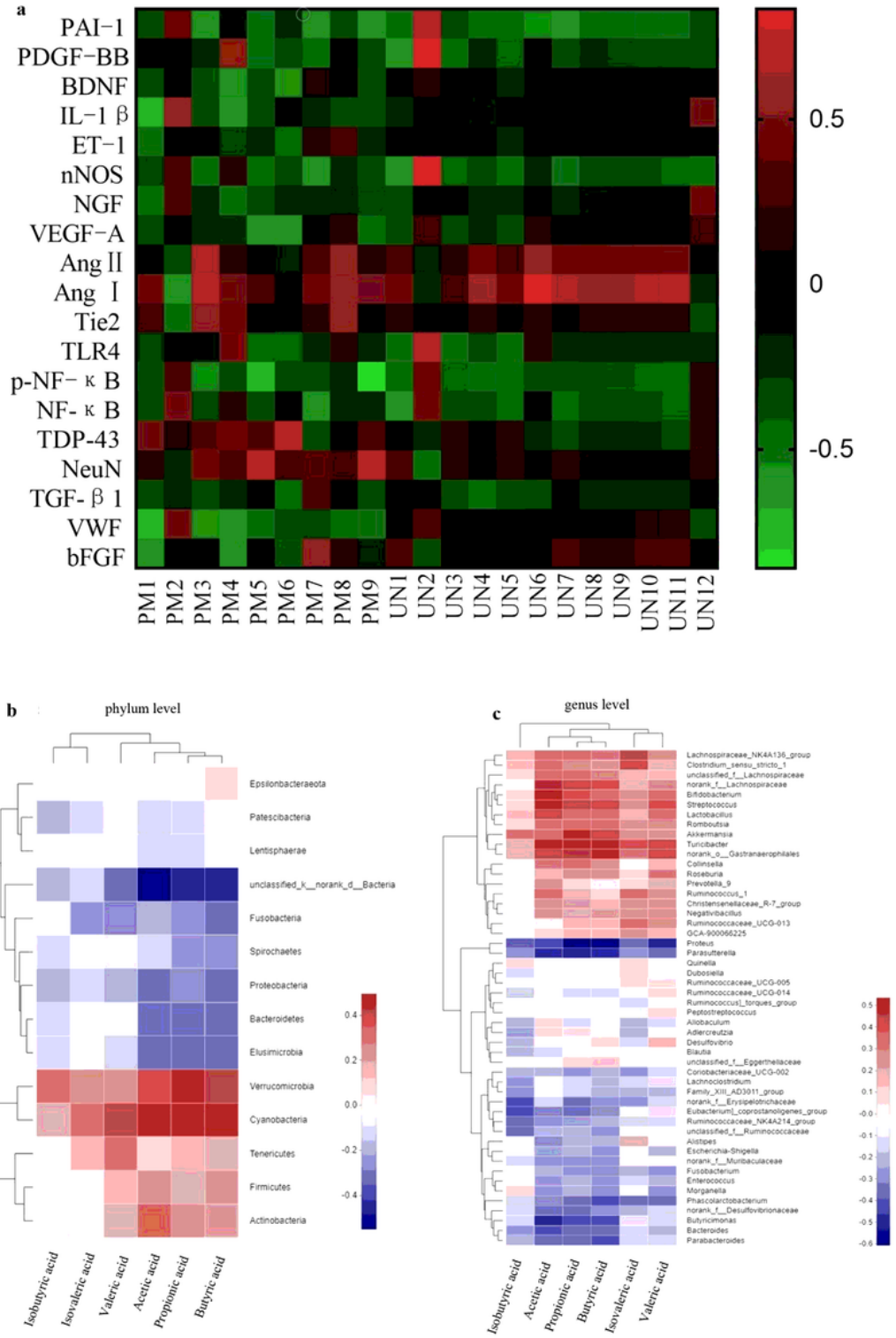

Figure 5

Heat map analysis of potential biomarkers and biochemical indicators (a); Heat map analysis of intestinal microflora and short-chain fatty acids at phylum level (b) and genus level (c).

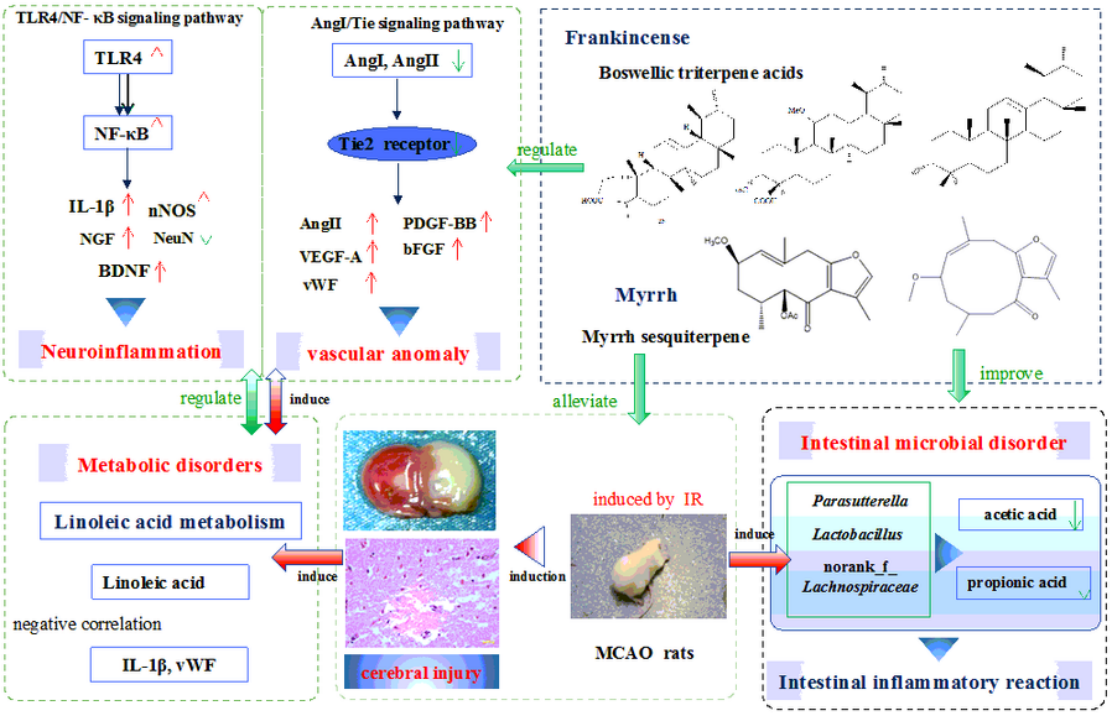

Figure 6

The mechanisms of BA-MS for regulating biochemical indexes, metabolic disorders and intestinal microbial disorders in MCAO rats.

Supplementary Files

This is a list of supplementary files associated with this preprint. Click to download.

- supplementary.docx